Bound and scattering state energies of Hulthén-Hellmann potential with external field and topological defects

U. S. Okorie[a], G. J. Rampho[a] and A. N. Ikot[b,c]

[a]*Department of Physics, University of South Africa, Florida, 1710, Johannesburg, South Africa*
e-mail: okoriu@unisa.ac.za
[b]*Theoretical Physics Group, Department of Physics, University of Port Harcourt, Rivers State, Nigeria.*
e-mails: ramphjg@unisa.ac.za; ndemikotphysics@gmail.com
[c]*Western Caspian University Baku, Azerbaijan.*

Received 10 March 2025; accepted 26 June 2025

Topological defect and external fields influence on potential models has been significantly proven to shape the behaviour and interactions of different constituent quantum systems. Due on this fact, we employ the Nikiforov-Uvarov functional analysis method to solve the Schrödinger equation with Hulthén-Hellmann Potential, embedded with Aharonov-Bohm flux field and point-like global monopole defect. Analytical expression of the energies with topological defect and AB flus field was obtained. In addition, the scattering phase shift expression of the combined potential was obtained under the influence of the global monopole and external field. Numerical and graphical variations have been presented for various quantum states, flux field and topological defect values. It is observed that, energy eigenvalues and scattering phase shift of the combined potential are significantly affected by the topological defect parameters, Aharonov-Bohm flux field, screening parameter and quantum state values considered, in the curved space-time. Conventional results of this study in Minkowski space-time are realized as the topological defect parameter approaches unity, in the absence of the AB flux field and these results agree with available results in literature. The results in this study also point relatively to some physical phenomena in chemical and molecular physics.

Keywords: Bound state; scattering state; combined potential; topological defect.

DOI: https://doi.org/10.31349/RevMexFis.71.060502

1. Introduction

For several decades now, different studies has been carried out with various wave equations in the presence of numerous curvature and torsional space-times. This concept by implication in a curved space-time has resulted in what is known as topological defects [1–7]. The topological defects generally are known to occur in condensed matter physics and gravitation physics. In gravitation physics, the concepts of topological defects were observed in the evolution of the early universe where symmetry breaking phase transition occurs [8, 9] while topological defects were observed in material synthesis in condensed matter physics [10, 11].

Some authors have investigated the relativistic oscillators with different topological defects [12–15]. Lambaga and Ramadhan [16] was investigated the global monopole with harmonic oscillator within the nonrelativistic quantum mechanics. Boumali and Aounallah [17] obtained the exact solutions of scalar bosons with Aharonov-Bohm (AB) and Coulomb potentials in the presence of global monopole. The effect of topological defects with Dirac and Klein-Gordon oscillators were investigated within the global monopole space-time environment [18]. Vitoria and Belich [19] recently employed the cosmic strings topological defects in Einstein equation to describe the global monopole point-like defects in solids. Within an elastic medium, the effect of declination topological defect on the interaction of a spinless electron with radial electric fields was investigated by Bakke and Furtado [20]. The effect of screw dislocation on electrons confined in both deformed Kratzer potential and pseudoharmonic quantum dot, respectively, was considered under the influence of an external magnetic field [21, 22].

In addition, Santos and Barros Jr. [23] considered the non-inertial effects of Klein-Gordon oscillator in the cosmic string space-time. Ahmed [24] also investigated the Klein-Gordon oscillator with linear potential in the background of cosmic string space-time, using the Kaluza-Klein theory. Bouzenada *et al*. [25] studied the effect of cosmic string and magnetic field on different thermal properties of a 2-dimensional Klein-Gordon oscillator, using the Poisson approximation. The influence of oscillatory frequency in a non-inertial system of Dirac oscillator was investigated in the cosmic string space-time background [26]. The authors obtained Dirac spinors for positive-energies nonrelativistic energies, which were compared with the confinement of a spin-half particle to quantum dot. Bakke and Furtado [27] analyzed the influence of Aharonov-Casher effect on the Dirac oscillator in Minkowski, cosmic string and cosmic dislocation space-times. Their study was applied to relativistic quantum dots, especially neutral particles. The influenced of topological defects on the magnetization and persistent current of massless Dirac fermions with quantum dot in a graphene layer were considered [28]. Here, the Dirac fermions were seen to contribute to the spatial confinement of electrons, and the degeneracy of the Landau levels being broken by the topological defects. Bakke and Mota [29] employed the gravity's rainbow to study the Dirac oscillator within the cosmic string space-time. They deduced that the energy levels of the Dirac oscillator were altered, due to the modification of the cosmic strings line elements by the rainbow functions. Also, the Kratzer and screened modified Kratzer potentials have been studied in a global monopole space-time [30]. It was discovered that the topological defect has some notable influence on their effective potentials and energy spectra. Chakraborty *et al*. [31] examined the screening of an external Coulomb charge with topological defects. They showed the dependence of the polarization charge on Coulomb strength and the effect of the conical defect indicates the topological defect dependence on the Coulomb charge. Other studies on effects of topological defect on thermal, magnetic and optical properties of some potential models have been recently considered, as recorded in Refs. [32–36].

The studies of the scattering state phase shift in recent times with confining potential models have been greatly appreciated in the areas of particle and nuclear physics, especially in cross-sectional phenomena for nuclear structures [37, 38]. Here, different wave functions of the systems under study have been decomposed into partial waves, with their unique angular momentum [39]. These concept has also been studied in relation to topological defects [40–42]. Recently, Alves *et al*. [43] studied the influence of electron by the Hulthén potential in a space-time containing a topological defect. Approximate solution for the scattering phase shift and the s-matrix were obtained for the Hulthén problem, in addition to the bound state solutions.

It has been established that the superposition of two or more potential model leads to broader range of applications [44, 45]. Hence, the Hulthén plus Hellmann potential (HHP), which is of interest to us is given as [46]

$$V_{HHP}(r) = -\frac{H_1 e^{-\delta r}}{1-e^{-\delta r}} + \frac{H_2 e^{-\delta r}}{r} - \frac{H_3}{r}. \tag{1}$$

Here, H_1, H_2, H_3 are depths of the combined potential and δ the screening parameter, respectively. The HHP model promises to be very relevant in different areas of physics including nuclear and particle physics, atomic and molecular physics, solid state physics and plasma physics. This is because, the Hulthén potential, Coulomb potential and Yukawa potential are special cases of the HHP [47].

2. Non-relativistic quantum energies in the global monopole space-time

2.1. Bound States

The line element with a point-like global monopole (PGM) space-time is defined as

$$ds^2 = -c^2dt^2 + \frac{dr^2}{\alpha^2} + r^2d\theta^2 + r^2\sin^2\theta d\varphi^2, \tag{2}$$

where $0 < \alpha^2 < 1$, $\alpha = 1 - 8\pi G\eta_0^2$, with α and η_0 being the topological effect parameter of the PGM and the energy scale, respectively and c is the speed of light. The metrics given in Eq. (2) describes a space-time with scalar curvature $R = 2(1-\alpha^2)/r^2$. The Schrödinger equation (SE) in this context is given as

$$-\frac{\hbar^2}{2\mu}\nabla_{LB}^2\psi(\vec{r},t) + V(\vec{r},t)\psi(\vec{r},t) = i\hbar\frac{\partial\psi(\vec{r},t)}{\partial t}, \tag{3}$$

where μ is the reduced mass of the system and $\nabla_{LB}^2 = (1/\sqrt{g})\partial_i\left(\sqrt{g}g^{ij}\partial_i\right)$ is the Laplace-Beltrami operator, $g = \det(g_{ij}) = r^2\sin^2\theta/\alpha^2$ and $V(r)$ is given in Eq. (1). Hence, the SE in the presence of the PGM and AB flux field is given as

$$\frac{-\hbar^2}{2\mu r^2}\left[\alpha^2\frac{\partial}{\partial r}\left(r^2\frac{\partial}{\partial r}\right) + \frac{1}{\sin\theta}\frac{\partial}{\partial\theta}\left(\sin\theta\frac{\partial}{\partial\theta}\right) + \frac{1}{\sin^2\theta}\frac{\partial^2}{\partial\varphi^2}\right]\psi(r,\theta,\varphi,t) + V_{HHP}(r)\psi(r,\theta,\varphi,t) = i\hbar\frac{\partial\psi(r,\theta,\varphi,t)}{\partial t}. \tag{4}$$

By considering a particular solution of Eq. (4) given in terms of eigenvalues of the angular momentum operator $\hat{L}^2$,

$$\psi(r,\theta,\varphi,t) = \exp\left(\frac{-iE_{nl}t}{\hbar}\right)\frac{R_{nl}(r)}{r}Y_{l,m}(\theta,\varphi), \tag{5}$$

where $Y_{l,m}(\theta,\varphi)$ are spherical harmonics and $R_{nl}(r)$ is the radial wave function. By substituting Eqs. (5) and (1) into Eq. (4), we have

$$\frac{d^2R_{nl}(r)}{dr^2} + \left[\frac{2ME_{nl}}{\hbar^2\alpha^2} + \frac{2\mu H_1 e^{-\delta r}}{\hbar^2\alpha^2(1-e^{-\delta r})} - \frac{2\mu H_2\delta e^{-\delta r}}{\hbar^2\alpha^2 r} + \frac{2\mu H_3\delta}{\hbar^2\alpha^2 r} - \frac{(l-\phi)(l-\phi+1)}{\alpha^2 r^2}\right]R_{nl}(r) = 0, \tag{6}$$

where l and ϕ represent angular momentum quantum number and AB flux field, respectively.

It has been established in available literatures that Eq. (6) does not have analytical solutions because of the presence of the centrifugal barrier, except for the s-wave where $l = 0$. Hence, we employ the Greene-Aldrich approximation scheme of the form [48],

$$\frac{1}{r^2} \approx \frac{\delta^2}{(1-e^{-\delta r})^2}; \frac{1}{r} \approx \frac{\delta}{(1-e^{-\delta r})}, \tag{7}$$

By substituting Eq. (7) into Eq. (6) and adopting a coordinate transformation $y = e^{-\delta r}$, we obtain

$$\frac{d^2 R_{nl}(y)}{dy^2} + \frac{1}{y}\frac{dR_{nl}(y)}{dy} + \left[\frac{-L_1 y^2 + L_2 y - L_3}{y^2(1-y)^2}\right] R_{nl}(y) = 0. \tag{8}$$

Here, the following parameters have been defined:

$$L_1 = \epsilon_{nl} + \frac{2\mu H_1}{\hbar^2\alpha^2\delta^2} - \frac{2\mu H_2}{\hbar^2\alpha^2\delta}; \qquad L_2 = 2\epsilon_{nl} + \frac{2\mu H_1}{\hbar^2\alpha^2\delta^2} - \frac{2\mu H_2}{\hbar^2\alpha^2\delta} - \frac{2\mu H_3}{\hbar^2\alpha^2\delta};$$

$$L_3 = \epsilon_{nl} - \frac{2\mu H_3}{\hbar^2\alpha^2\delta} + \frac{(l-\psi)(l-\psi+1)}{\alpha^2}; \qquad \epsilon_{nl} = \frac{-2\mu E_{nl}}{\hbar^2\alpha^2\delta^2}. \tag{9}$$

To get the bound state solution, one can see that as $R_{nl}(r) \to 0, y \to 0$ when $r \to \infty$ and $y \to 1$ when $r \to 0$. Thus, we employ the wave function of the form,

$$R_{nl}(y) = y^S (1-y)^Q F_{nl}(y) \tag{10}$$

Substituting Eq. (10) into Eq. (8) and using the NUFA method as summarized in the Appendix A, we obtain S and Q as,

$$S = \sqrt{\frac{(l-\phi)(l-\phi+1)}{\alpha^2} - \frac{2\mu H_3}{\hbar^2\alpha^2\delta} - \frac{2\mu E_{nl}}{\hbar^2\alpha^2\delta^2}}, \tag{11}$$

$$Q = \frac{1}{2}\left(1 + \sqrt{1 + \frac{4(l-\phi)(l-\phi+1)}{\alpha^2}}\right). \tag{12}$$

The bound state energy spectrum for the HHP with with PGM and AB flux field can be obtained using Eq. (A.15) as,

$$E_{nl} = \frac{\hbar^2\alpha^2\delta^2}{2\mu}\left(\frac{(l-\phi)(l-\phi+1)}{\alpha^2} - \frac{2\mu H_3}{\hbar^2\alpha^2\delta}\right) - \frac{\hbar^2\alpha^2\delta^2}{2\mu}$$
$$\times\left[\frac{(n+Q)}{2} - \frac{\left(\frac{2\mu H_1}{\hbar^2\alpha^2\delta^2} - \frac{2\mu H_2}{\hbar^2\alpha^2\delta} + \frac{2\mu H_3}{\hbar^2\alpha^2\delta} - \frac{(l-\phi)(l-\phi+1)}{\alpha^2}\right)}{2\,(n+Q)}\right]^2. \tag{13}$$

The corresponding wave function can be obtained using Eqs. (11) and (12) as,

$$R_{nl}(r) = N_{nl}\left(e^{-\delta r}\right)^S \left(1 - e^{-\delta r}\right)^Q {}_2F_1(a,b,c;z), \tag{14}$$

where N_{nl} is the normalization constant. In terms of Jacobi polynomials, we have

$$R_{nl}(r) = N_{nl}\left(e^{-\delta r}\right)^S \left(1 - e^{-\delta r}\right)^Q P_n^{(2S,2Q-1)}\left(1 - 2e^{-\delta r}\right). \tag{15}$$

To obtain the normalization constant, the normalization condition of the radial wave function is employed:

$$\int_0^\infty |R_{nl}(r)|^2\, dr = 1. \tag{16}$$

Considering the condition at $r \in (0,\infty)$ and $e^{-\delta r} \in (1,0)$, we have

$$\frac{N_{nl}^2}{\delta}\int_1^0 y^{2S}(1-y)^{2Q}\left[P_n^{(2S,2Q-1)}(1-2y)\right]^2 \frac{dy}{y} = 1, \qquad \left(y = e^{-\delta r}\right). \tag{17}$$

By using the transformation $\eta = 1 - 2y$, we have the following boundary of Eq. (17) change from $y \in (1,0)$ to $\eta \in (-1,1)$. This gives

$$\frac{N_{nl}^2}{2\delta}\int_{-1}^1 \left(\frac{1-\eta}{2}\right)^{2S-1}\left(\frac{1+\eta}{2}\right)^{2Q}\left[P_n^{(2S,2Q-1)}(\eta)\right]^2 d\eta = 1. \tag{18}$$

From the standard integral formula [52],

$$\int_{-1}^1 \left(\frac{1-q}{2}\right)^\omega \left(\frac{1+q}{2}\right)^z \left[P_n^{(\omega,z-1)}(\eta)\right]^2 dq = \frac{2^{\omega+z+1}\Gamma(1+n+\omega)\Gamma(1+n+z)}{n!\Gamma(1+n+\omega+z)\Gamma(1+2n+\omega+z)}. \tag{19}$$

By comparing Eqs. (18) and (19), the normalization constant becomes

$$N_{nl} = \sqrt{\frac{2\delta(n!)\Gamma(n+2S+2Q)\Gamma(2n+2S+2Q)}{2^{2S+2Q}\Gamma(n+2S)\Gamma(1+n+2Q)}}. \tag{20}$$

The total wave function for the Hulthén plus Hellmann potential with AB flux field and point-like global monopole now becomes

$$R_{nl}(r) = \sqrt{\frac{2\delta(n!)\Gamma(n+2S+2Q)\Gamma(2n+2S+2Q)}{2^{2S+2Q}\Gamma(n+2S)\Gamma(1+n+2Q)}} \left(e^{-\delta r}\right)^S \left(1-e^{-\delta r}\right)^Q P_n^{(2S,2Q-1)}\left(1-2e^{-\delta r}\right). \tag{21}$$

2.2. Scattering states

In this section, we proceed to study the scattering state Schrödinger equation of HHP within the AB flux field and global monopole space-time framework. By substituting Eq. (7) into Eq. (6) with a new coordinate transformation of the form $\sigma = (1-e^{-\delta r})$, we have

$$\sigma(1-\sigma)\frac{d^2R_{nl}(\sigma)}{d\sigma^2} - \sigma\frac{dR_{nl}(\sigma)}{d\sigma} + \left[\frac{G_1+G_2\sigma+G_3\sigma^2}{\sigma(1-\sigma)}\right]R_{nl}(\sigma) = 0, \tag{22}$$

where,

$$G_1 = -\frac{(l-\phi)(l-\phi+1)}{\alpha^2}, \qquad G_2 = \frac{2\mu H_1}{\hbar^2\alpha^2\delta^2} - \frac{2\mu H_2}{\hbar^2\alpha^2\delta} + \frac{2\mu H_3}{\hbar^2\alpha^2\delta}, \qquad G_3 = \frac{2\mu E_{nl}}{\hbar^2\alpha^2\delta^2} - \frac{2\mu H_1}{\hbar^2\alpha^2\delta^2} + \frac{2\mu H_2}{\hbar^2\alpha^2\delta}. \tag{23}$$

Equation (22) has regular singularities at $\sigma = 0, 1$ and ∞. Therefore $R(\sigma=0) = 0$ as $r \to \infty$ and $R(\sigma=0) = 1$ as $r \to 0$. Thus, the wave function can be written in the form,

$$R_{nl}(\sigma) = \sigma^{\lambda}(1-\sigma)^{\frac{-it}{\delta}}\xi_{nl}(\sigma), \tag{24}$$

where,

$$\lambda = \frac{1}{2}\left(1 \pm \sqrt{1-4G_1}\right); t = \delta\sqrt{G_1+G_2+G_3}. \tag{25}$$

Substituting Eq. (24) into Eq. (22) gives the hypergeometric Gauss differential equation of the form

$$\sigma(1-\sigma)\frac{d^2\xi}{d\sigma^2} + \left[2\lambda - (1-\frac{2it}{\delta})\sigma\right]\frac{d\xi}{d\sigma} + \left(\lambda - \frac{it}{\delta} + \sqrt{-G_3}\right)\left(\lambda - \frac{it}{\delta} - \sqrt{-G_3}\right)\xi(\sigma) = 0. \tag{26}$$

The solution of Eq. (26) is the hypergeometric function given as

$$\xi_{nl}(\sigma) = {}_2F_1\left(\Xi_1, \Xi_2, \Xi_3; \sigma\right), \tag{27}$$

where,

$$\Xi_1 = \left(\lambda - \frac{it}{\delta} + \sqrt{-G_3}\right), \qquad \Xi_2 = \left(\lambda - \frac{it}{\delta} - \sqrt{-G_3}\right), \qquad \Xi_3 = 2\lambda, \tag{28}$$

By using Eqs. (25) and (27), we obtain the scattering wave function as

$$R_{nl}(\sigma) = \sigma^{\lambda}(1-\sigma)^{\frac{-it}{\delta}}\ {}_2F_1\left(\Xi_1, \Xi_2, \Xi_3; \sigma\right). \tag{29}$$

To obtain to the scattering phase shift, we used the following asymptotic properties [53]. As $R_{nl}(\sigma) \to 0$, $\sigma \to 0$, Eq. (29) becomes

$$R_{nl}(\sigma) \to 2\sin\left[t\sigma + J - \frac{l\pi}{2} + \frac{\pi(l+1)}{2}\right], \quad \sigma \to \infty, \tag{30}$$

where J is the scattering phase shift. The phase shift can be obtained from Eq. (30) as follows

$$J_l = \frac{\pi(l+1)}{2} + \arg\Gamma\left(\Xi_3 - \Xi_2 - \Xi_1\right) - \arg\Gamma\left(\Xi_3 - \Xi_2\right) - \arg\Gamma\left(\Xi_3 - \Xi_1\right). \tag{31}$$

It is worthy to mention here that the details for the derivation of phase shift factor is presented in Ref. [54]. By using Eq. (28), Eq. (31) can be written as,

$$J_l = \frac{\pi(l+1)}{2} + \arg\Gamma\left(\frac{2it}{\delta}\right) - \arg\Gamma\left(\lambda - \frac{it}{\delta} - \sqrt{-G_3}\right) - \arg\Gamma\left(\lambda - \frac{it}{\delta} + \sqrt{-G_3}\right). \tag{32}$$

TABLE I. Bound state energy eigenvalues (eV) of the HHP at different values of quantum states, topological defect and AB flux field.

n	l	$\phi = 1.0$			$\phi = 2.0$			$\phi = 3.0$		
		$\alpha = 0.25$	$\alpha = 0.65$	$\alpha = 0.85$	$\alpha = 0.25$	$\alpha = 0.65$	$\alpha = 0.85$	$\alpha = 0.25$	$\alpha = 0.65$	$\alpha = 0.85$
0	0	-35.9875098	-5.3130098	-3.1017997	-0.8990078	-0.6770681	-0.5890331	-0.2922768	-0.2466045	-0.2265672
1	0	-8.9875391	-1.3191250	-0.7664983	-0.6628190	-0.3574311	-0.2753900	-0.2408371	-0.1584860	-0.1313853
	1	-8.9875391	-1.3191250	-0.7664983	-8.9875391	-1.3191250	-0.7664983	-0.6628190	-0.3574311	-0.2753900
2	0	-3.9875879	-0.5798101	-0.3345368	-0.5078996	-0.2182803	-0.1566163	-0.2014847	-0.1092836	-0.0844516
	1	-3.9875879	-0.5798101	-0.3345368	-3.9875879	-0.5798101	-0.3345368	-0.5078996	-0.2182803	-0.1566163
	2	-0.5078996	-0.2182803	-0.1566163	-3.9875879	-0.5798101	-0.3345368	-3.9875879	-0.5798101	-0.3345368
3	0	-2.2376563	-0.3213965	-0.1839429	-0.4008613	-0.1457484	-0.0997541	-0.1707333	-0.0792978	-0.0583731
	1	-2.2376563	-0.3213965	-0.1839429	-2.2376563	-0.3213965	-0.1839429	-0.4008613	-0.1457484	-0.0997541
	2	-0.4008613	-0.1457484	-0.0997541	-2.2376563	-0.3213965	-0.1839429	-2.2376563	-0.3213965	-0.1839429
	3	-0.1707332	-0.0792978	-0.0583731	-0.4008613	-0.1457484	-0.0997540	-2.2376563	-0.3213965	-0.1839429
4	0	-1.4277441	-0.2021681	-0.1148897	-0.3238577	-0.1034766	-0.0686693	-0.1462704	-0.0599162	-0.0428310
	1	-1.4277441	-0.2021681	-0.1148897	-1.4277441	-0.2021681	-0.1148897	-0.3238577	-0.1034766	-0.0686693
	2	-0.3238577	-0.1034766	-0.0686693	-1.4277441	-0.2021681	-0.1148897	-1.4277441	-0.2021681	-0.1148897
	3	-0.1462704	-0.0599162	-0.0428310	-0.3238577	-0.1034766	-0.0686693	-1.4277441	-0.2021681	-0.1148897
	4	-0.0734979	-0.0345933	-0.0261698	-0.1462704	-0.0599162	-0.0428310	-0.3238577	-0.1034766	-0.0686693
5	0	-0.9878516	-0.1378056	-0.0780693	-0.2666467	-0.0769464	-0.0502783	-0.1265129	-0.0468885	-0.0332356
	1	-0.9878516	-0.1378056	-0.0780693	-0.9878516	-0.1378056	-0.0780693	-0.2666467	-0.0769464	-0.0502783
	2	-0.2666467	-0.0769464	-0.0502783	-0.9878516	-0.1378056	-0.0780693	-0.9878516	-0.1378056	-0.0780693
	3	-0.1265129	-0.0468885	-0.0332356	-0.2666467	-0.0769464	-0.0502783	-0.9878516	-0.1378056	-0.0780693
	4	-0.0651682	-0.0281489	-0.0215037	-0.1265129	-0.0468885	-0.0332356	-0.2666467	-0.0769464	-0.0502783
	5	-0.0322698	-0.0154562	-0.0129736	-0.0651682	-0.0281489	-0.0215037	-0.1265129	-0.0468885	-0.0332356

3. Results and discussions

In this section, the energy spectrum of Hulthén-Hellmann potential obtained in Eq. (13) is analyzed with different potential parameters, under the influence of AB flux field ϕ and topological defect parameter α. The combined potential parameters and arbitrary constants employed are as follows: $H_1 = 0.025; H_2 = -1.00; H_3 = 1.00; \hbar = 1; \mu = 0.5$. The values of the energy for HHP are seen to increase with increase in quantum state for any value of topological defect and AB flux field considered. It can be observed that the there exist a significant increase in the energy eigenvalues from ground state of the exited states of the system. This is illustrated in Table I. At each quantum state considered, the energy eigenvalues of HHP increases with increase in both topological defect and AB flux field values. The increase in energy eigenvalues at each quantum state considered is not as significant as that observed between different quantum states. hence, we see that under the dominance of AB flux field, the energy eigenvalues of HHP are enhanced in the presence of the topological defects. In addition, there exist inter-AB flux field degeneracy symmetry $(E_l^{\phi} = E_{l+1}^{\phi+1})$ at specific values of topological defect. Hence, the bound state energy eigenvalues for HHP is invariant under a transformation of an in-

TABLE II. Comparison of Bound state energy eigenvalues eV of the HHP for Minkowski flat space, in the absence of AB flux field, at different values of quantum states, with $\delta = 0.025$.

n	l	$\phi = 0; \alpha = 1.0$	[46]
0	0	-2.23765625	-2.2376562500
1	0	-0.55062500	-0.5506250000
	1	-0.23001736	-0.2300173611
2	0	-0.23890625	-0.2389062500
	1	-0.12535156	-0.1253515625
	2	-0.07075625	
3	0	-0.13062500	-0.13062500000
	1	-0.07780625	
	2	-0.04765625	
	3	-0.02860013	
4	0	-0.08140625	
	1	-0.05293403	
	2	-0.03472258	
	3	-0.02222656	
	4	-0.01319637	

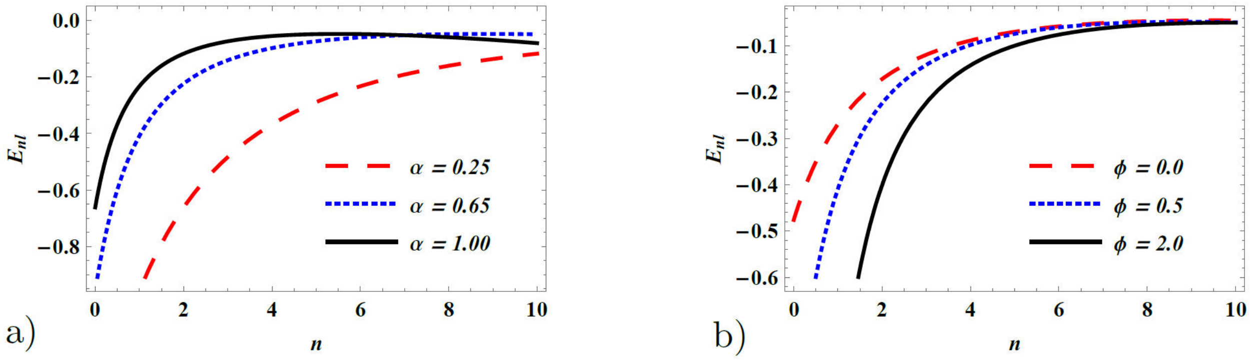

FIGURE 1. Variation of energy eigenvalues of HHP with principal quantum number n for various values of a) topological defect α; b) AB flux field ϕ.

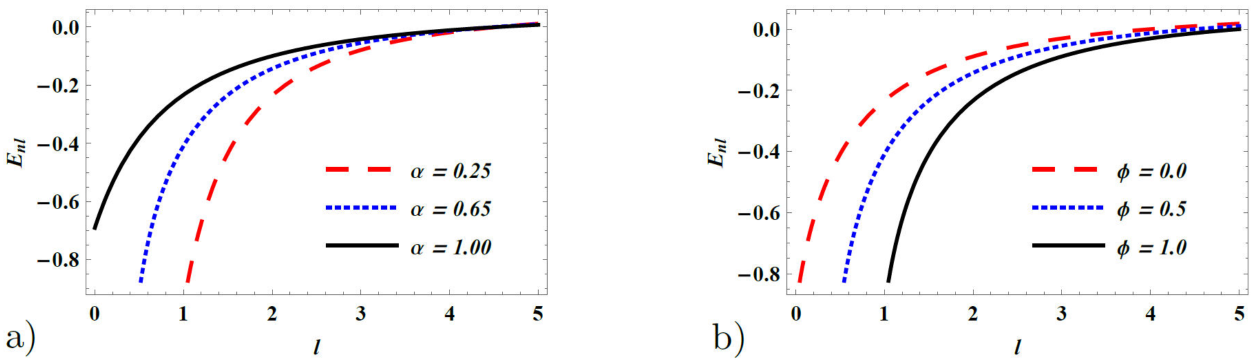

FIGURE 2. Variation of energy eigenvalues of HHP with angular momentum quantum number l for various values of a) topological defect α; b) AB flux field ϕ.

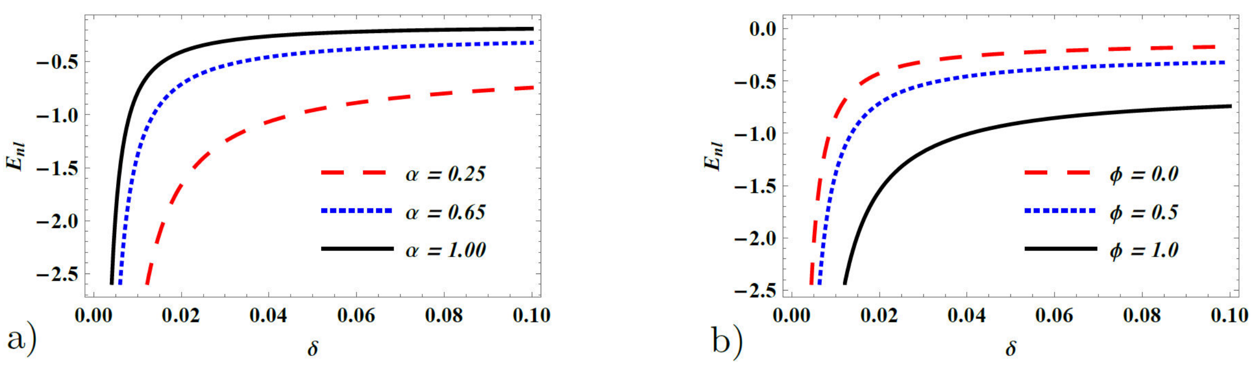

FIGURE 3. Variation of energy eigenvalues of HHP with screening parameter δ for various values of a) topological defect α; b) AB flux field ϕ.

crease in the AB flux field by one ($\phi \rightarrow \phi + 1$) and an increase in the angular momentum quantum number by one ($l \rightarrow l + 1$), at each principal quantum number and topological defect values considered.

Table II shows the bound state energy eigenvalues of HHP for Minkowski flat space at different quantum states. Our results are seen to be very consistent with the results obtained in Ref. [43].

The graphical relationship between the energy eigenvalues of HHP with quantum numbers and screening parameter, for some values of topological defect and AB flux field are presented in Figs. 1-4. In Fig. 1a), the energy eigenvalues are seen to rise monotonously with increase in principal quantum number n, for varying values of topological defect α. As the n is enhanced more, the energy curves for the various topological defect are seen to converge. Also, the energies of HHP increase with increase in topological defect values, at any values of n considered. We also observe a convergence in the energy curves of HHP for greater values of n, as shown in Fig. 1b). Conversely, the energies of HHP increase with a decrease in AB flux field values, for any value of n.

In Fig. 2a), the energy eigenvalues are seen to rise monotonously with increase in angular momentum quantum number l, for varying values of topological defect α. As the l is enhanced more, the energy curves for the various topological defect are seen to converge. Also, the energies of HHP

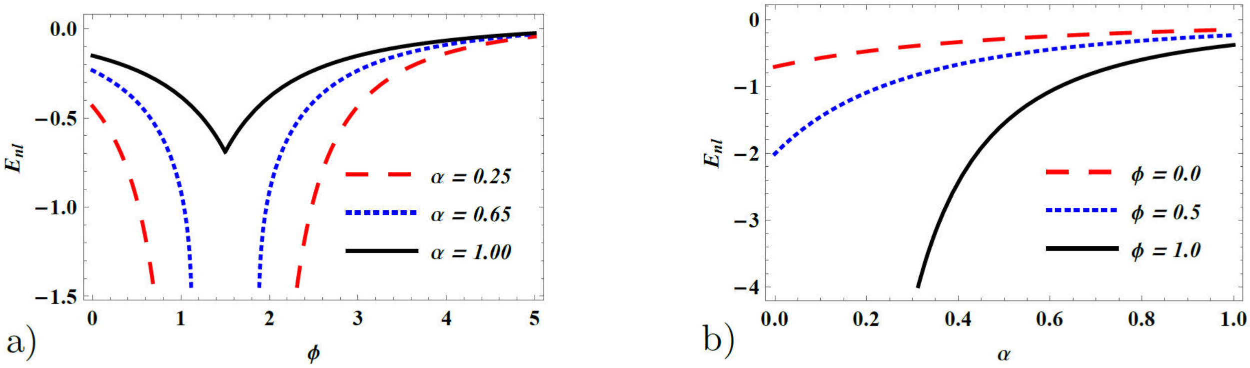

FIGURE 4. Variation of energy eigenvalues of HHP with a) AB flux field ϕ for various values topological defect α; b) topological defect α for various values of AB flux field ϕ.

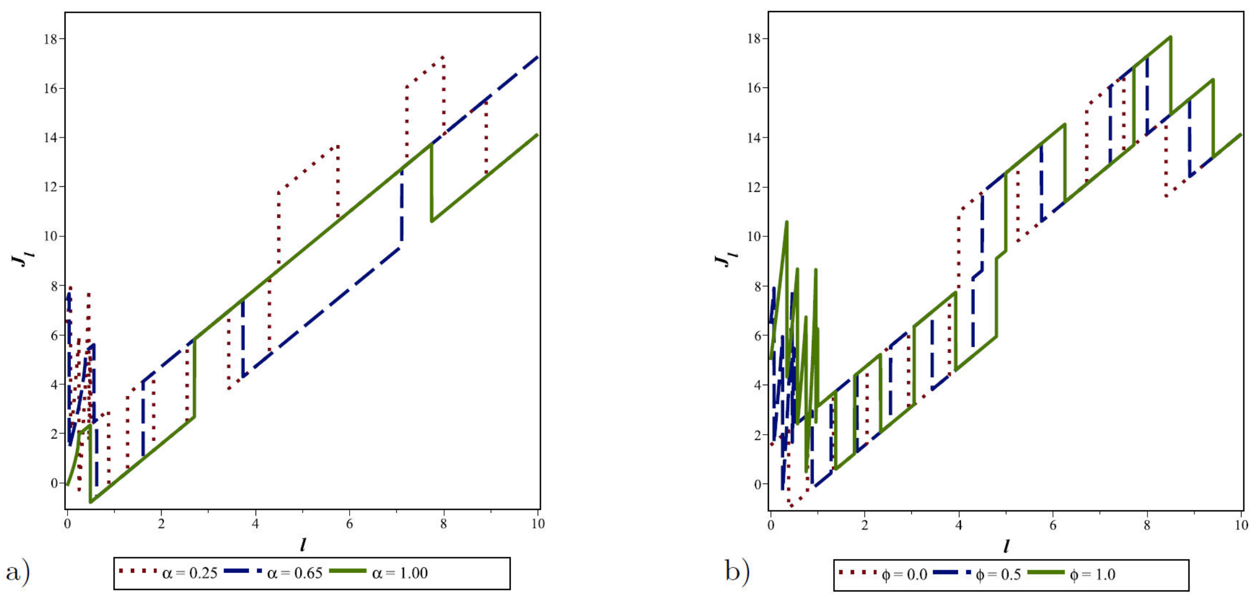

FIGURE 5. Variation of scattering phase shift of HHP with angular momentum quantum number for various values of a) topological defect α; b) AB flux field ϕ.

increase with increase in topological defect values, at any values of l considered. We also observe a convergence in the energy curves of HHP for greater values of l, as shown in Fig. 2b). Conversely, the energies of HHP increase with a decrease in AB flux field values, for any value of l.

In Fig. 3a), the energy eigenvalues increase slowly with increase in the screening parameter δ, for varying values of topological defect α. As δ is enhanced more, the energy curves for the various topological defect are seen to remain constant. Also, the energies of HHP increase with increase in topological defect values, at any values of δ considered. The same trend is also observe in Fig. 3b) for various values of AB flux field considered. Also, the energies of HHP increase with a decrease in AB flux field values, for any value of δ. It can be deduced that the energies of the HHP are mostly influenced at lower values of screening parameter, irrespective of the values of the topological defect and AB flux field considered.

The variation of the energy eigenvalues of HHP with AB flux field (ϕ) is shown in Fig. 4a), for various values of topological defect (α). Here, the energy curves decrease uniquely to a point and later increase as the AB flux field is enhanced. The fall and rise levels of the energies corresponds inversely to the level of topological defects considered.

The graphical relationship between the scattering phase shift of HHP with angular momentum quantum number, for some values of topological defect and AB flux field are presented in Figs. 5-6. In Fig. 5a), we observe a unique sawtooth-like behaviour of the scattering phase shift for increasing energy eigenvalues, corresponding to each value of topological defect considered. For lower values of l, the scattering phase shift is seen to be more dense, as compared to the scattering phase shift at higher values of l. In Fig. 5b), we also observe a more dense scattering phase shift at lower l, for various values of AB flux field ϕ. As l is enhanced the more, the scattering phase shift increases in a sawtooth form,

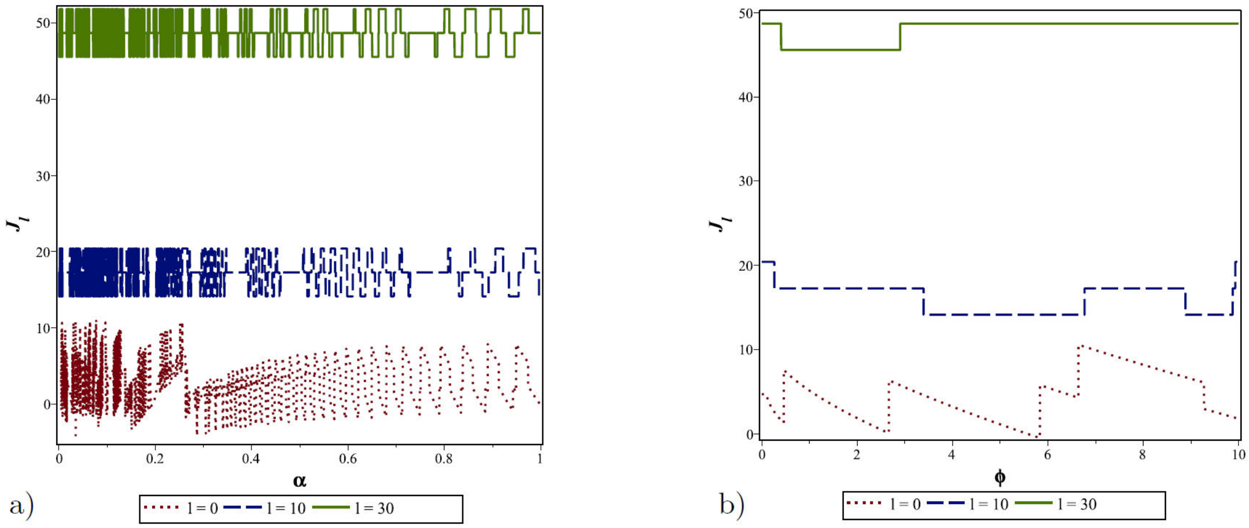

FIGURE 6. Variation of scattering phase shift of HHP with a) topological defect α, for various values of angular momentum quantum number b) AB flux field ϕ, for various values of angular momentum quantum number.

for the various values of ϕ considered. In both cases, the scattering phase shift increases linearly with increasing l.

In Fig. 6a), the scattering phase shift of HHP is varied with topological defect, for various values of angular momentum quantum number at a fixed value of AB flux field. It can be observed that the scattering phase shift is more dense at a region of lower values of topological defect (α). As α increases, the scattering phase shift begins to space out. The scattering phase shift occurs spreads out within a specified range for each value of l considered. In Fig. 6b), the variation of the scattering phase shift with AB flux field takes different unique natures, corresponding to each value of l considered. These curves occurs in different ranges as l increases. It can also be confirmed in these figures that the scattering phase shift increases with increase in angular momentum quantum number.

4. Conclusion

Topological defects on the eigensolutions of Hulthén-Hellmann potential have been studied in this work under the framework of Nikiforov-Uvarov functional analysis method. Greene-Aldrich approximation scheme has been employed to deal with the centrifugal term. Numerical values of the energy are presented in Table I for various quantum states (n and l) and AB flux fields (ϕ) in curved space ($0 < \alpha < 1$). The corresponding values of the energy in Minkowski flat space ($\alpha = 1$) and in the absence of the AB flux field ($\phi = 0$) are computed and compared with available results in literature, for some quantum states. This comparison are presented in Table II. It is observed that these results agree perfectly with each other, for a certain chosen arbitrary values of the potential parameters. It is also observed that the AB flux field in the curved space and fractional parameters considered have significant impact in the energy eigenvalues of the system under study. We have also seen that there exist inter-AB flux field degeneracy symmetry in the energy eigenvalues of HHP, at specific values of topological defect.

Graphical variations of the energy eigenvalues with quantum numbers and screening parameters, for varying values of AB flux field and topological defect are presented in Figs. 1-4. The significant influence of the topological defect and AB flux field which results in a shift in the energy eigenvalues of HHP, as demonstrated in the graphs are discussed clearly. In addition, the variation of scattering phase shift of HHP with angular momentum quantum number for varying topological defects and AB flux field, as presented in Figs. 5 and 6 are clearly discussed. The particles of the HHP are seen to be scattered more densely with lower values of angular momentum quantum number. Also, unique nature of sawtooth-like behaviour of the scattering phase shift are observed for each value of topological defect and AB flux field considered.

The vast application of our study has been shown in literatures. These includes condensed matter and atomic physics [49], high-energy physics with proton-proton scattering [50]. Here, the scattering amplitude of the particles are decomposed into various angular momentum corresponding to unique phase shifts. This concept can also be employed in quantum chromodynamics. In the area of acoustics, interference pattern of scattered waves can be affected by phase shift. This phenomenon is used in noise reduction [51].

It is our future intention to extend this work to spin-spin interaction, spin-orbit interactions, as they relate to heavy mesons. This is poised out of the fact that the combined potential with topological defects studied promises to be very efficient in atomic and nuclear physics and their related areas.

Appendix

A. Review of Nikiforov-Uvarov-Functional analysis method [52]

Using the concepts of NU method [53], parametric NU method [54] and the functional analysis method [55], we proposed a simple and elegant method for solving a second order differential equation of the hypergeometric type called Nikiforov-Uvarov-Functional Analysis (NUFA) method. As it is well-known, the NU is used to solve a second-order differential equation of the form [53]

$$\frac{d^2\psi(s)}{ds^2}+\frac{\tilde{\tau}(s)}{\sigma(s)}\frac{d\psi(s)}{ds}+\frac{\tilde{\sigma}(s)}{\sigma^2(s)}\psi(s)=0, \tag{A.1}$$

where $\sigma(s)$ and $\tilde{\sigma}(s)$ are polynomials, at most of second degree, and $\tilde{\tau}(s)$ is a first-degree polynomial. Tezcan and Sever [43] latter introduced the parametric form of NU method in the form

$$\frac{d^2\psi(s)}{ds^2}+\frac{\alpha_1-\alpha_2 s}{s(1-\alpha_3 s)}\frac{d\psi(s)}{ds}\frac{1}{s^2(1-\alpha_3 s)^2}\left[-\xi_1 s^2+\xi_2 s-\xi_3\right]\psi(s)=0, \tag{A.2}$$

where α_i and $\xi_i(i=1,2,3)$ are all parameters. It can be observed in Eq. (A.2) that the differential equation has two singularities at $s\to 0$ and $s\to 1/\alpha_3$, thus we take the wave function in the form,

$$\psi(s)=s^{\lambda}(1-\alpha_3 s)^{v}f(s). \tag{A.3}$$

Substituting Eq. (A.3) into Eq. (A.2) leads to the following equation,

$$\begin{aligned}&s(1-\alpha_3 s)\frac{d^2f(s)}{ds^2}+\left[\alpha_1+2\lambda-(2\lambda\alpha_3+2v\alpha_3+\alpha_2)s\right]\frac{df(s)}{ds}-\alpha_3\left(\lambda+v+\frac{1}{2}\left(\frac{\alpha_2}{\alpha_1}-1\right)+\sqrt{\frac{1}{2}\left(\frac{\alpha_2}{\alpha_1}^2+\frac{\xi_1}{\alpha_3^2}\right)}\right)\\&\times\left(\lambda+v+\frac{1}{2}\left(\frac{\alpha_2}{\alpha_1}-1\right)-\sqrt{\frac{1}{2}\left(\frac{\alpha_2}{\alpha_1}^2+\frac{\xi_1}{\alpha_3^2}\right)}\right)f(s)\\&+\left[\frac{\lambda(\lambda-1)+\alpha_1\lambda-\xi_3}{s}+\frac{v(v-1)\alpha_3+\alpha_2 v-\alpha_1\alpha_3 v-\frac{\xi_1}{\alpha_3+\xi_2-\xi_3\alpha_3}}{1-\alpha_3 s}\right]f(s)=0.\end{aligned} \tag{A.4}$$

Equation (A.4) can be reduced to a Gauss hypergeometric equation if and only if the following functions vanished,

$$\lambda(\lambda-1)+\alpha_1\lambda-\xi_3=0, \tag{A.5}$$

$$v(v-1)\alpha_3+\alpha_2 v-\alpha_1\alpha_3 v-\frac{\xi_1}{\alpha_3}+\xi_2-\xi_3\alpha_3=0. \tag{A.6}$$

Thus, Eq. (A.4) now becomes

$$\begin{aligned}&s(1-\alpha_3 s)\frac{d^2f(s)}{ds^2}+\left[\alpha_1+2\lambda-(2\lambda\alpha_3+2v\alpha_3+\alpha_2)s\right]\frac{df(s)}{ds}-\alpha_3\left(\lambda+v+\frac{1}{2}\left(\frac{\alpha_2}{\alpha_1}-1\right)+\sqrt{\frac{1}{2}\left(\frac{\alpha_2}{\alpha_1}^2+\frac{\xi_1}{\alpha_3^2}\right)}\right)\\&\times\left(\lambda+v+\frac{1}{2}\left(\frac{\alpha_2}{\alpha_1}-1\right)-\sqrt{\frac{1}{2}\left(\frac{\alpha_2}{\alpha_1}^2+\frac{\xi_1}{\alpha_3^2}\right)}\right)f(s)=0.\end{aligned} \tag{A.7}$$

Solving Eqs. (A.5) and A.6 completely give,

$$\lambda=\frac{1}{2}\left((1-\alpha_1)\pm\sqrt{(1-\alpha_1)^2+4\xi_3}\right), \tag{A.8}$$

$$v=\frac{1}{2\alpha_3}\left((\alpha_3+\alpha_1\alpha_3-\alpha_2)\pm\sqrt{(\alpha_3+\alpha_1\alpha_3-\alpha_2)^2+4\left(\frac{\xi_1}{\alpha_3}+\alpha_3\xi_3-\xi_2\right)}\right). \tag{A.9}$$

Equation (A.7) is the hypergeometric equation type of the form,

$$x(1-x)\frac{d^2f(x)}{dx^2}+\left[c+(a+b+1)x\right]\frac{df(x)}{dx}-(ab)f(x)=0, \tag{A.10}$$

where a, b, c are given as follows,

$$a = \sqrt{\alpha_3}\left(\lambda + v + \frac{1}{2}\left(\frac{\alpha_2}{\alpha_3} - 1\right) + \sqrt{\frac{1}{4}\left(\frac{\alpha_2}{\alpha_3} - 1\right)^2 + \frac{\xi_2}{\alpha_3^2}}\right), \tag{A.11}$$

$$b = \sqrt{\alpha_3}\left(\lambda + v + \frac{1}{2}\left(\frac{\alpha_2}{\alpha_3} - 1\right) - \sqrt{\frac{1}{4}\left(\frac{\alpha_2}{\alpha_3} - 1\right)^2 + \frac{\xi_2}{\alpha_3^2}}\right), \tag{A.12}$$

$$c = \alpha_1 + 2\lambda. \tag{A.13}$$

Setting either a or b equal to a negative integer $-n$, the hypergeometric function $f(s)$ turns to a polynomial of degree n. Hence, the hypergeometric function $f(s)$ approaches finite in the following quantum condition *i.e.* $a = -n$, where $n = 0, 1, 2, 3, ..., n_{\max}$. Using the above quantum condition,

$$\sqrt{\alpha_3}\left(\lambda + v + \frac{1}{2}\left(\frac{\alpha_2}{\alpha_3} - 1\right) + \sqrt{\frac{1}{4}\left(\frac{\alpha_2}{\alpha_3} - 1\right)^2 + \frac{\xi_2}{\alpha_3^2}}\right) = -n, \tag{A.14}$$

$$\lambda + v + \frac{1}{2}\left(\frac{\alpha_2}{\alpha_3} - 1\right) + \frac{n}{\sqrt{\alpha_3}} = -\sqrt{\frac{1}{4}\left(\frac{\alpha_2}{\alpha_3} - 1\right)^2 + \frac{\xi_2}{\alpha_3^2}}. \tag{A.15}$$

Squaring both sides of Eq. (A.15) and rearranging, we obtain the energy equation for the NUFA method as

$$\lambda^2 + 2\lambda\left(v + \frac{1}{2}\left(\frac{\alpha_2}{\alpha_3} - 1\right) + \frac{n}{\sqrt{\alpha_3}}\right) + \left(v + \frac{1}{2}\left(\frac{\alpha_2}{\alpha_3} - 1\right) + \frac{n}{\sqrt{\alpha_3}}\right)^2 - \frac{1}{4}\left(\frac{\alpha_2}{\alpha_3} - 1\right)^2 + \frac{\xi_2}{\alpha_3^2} = 0. \tag{A.16}$$

By substituting Eqs. (A.8) and (A.9) into Eq. (A.3), we obtain the corresponding wave equation for the NUFA method as

$$\psi(s) = \mathbb{N} s^{\frac{(1-\alpha_1)\pm\sqrt{(1-\alpha_1)^2+4\xi_3}}{2}} (1 - \alpha_3 s)^{(\alpha_3+\alpha_1\alpha_3-\alpha_2)\pm\sqrt{(\alpha_3+\alpha_1\alpha_3-\alpha_2)^2+4\left(\frac{\xi_1}{\alpha_3^2}+\alpha_3\xi_3-\xi_2\right)}} {}_2F_1(a, b, c; s), \tag{A.17}$$

where $\mathbb{N}$ is the normalization constant.

1. H. Hassanabadi, S. Zare, J. Kriz, and B. C. Lutfuoglu, *Electric quadrupole moment of a neutral non-relativistic particle in the presence of screw dislocation*, EPL **132** (2020) 60005. https://doi.org/10.1209/0295-5075/132/60005

2. S. Zare, H. Hassanabadi, and M. de Montigny, *Nonrelativistic particles in the presence of a Cariñena-Perelomov-Rañada-Santander oscillator and a disclination*, Int. J. Mod. Phys. A **35** (2020) 2050071. https://doi.org/10.1142/S0217751X20500712

3. W. C. F. da Silva, and K. Bakke, *Non-relativistic effects on the interaction of a point charge with a uniform magnetic field in the distortion of a vertical line into a vertical spiral spacetime*, Class. Quantum Grav. **36** (2019) 235002. https://doi.org/10.1088/1361-6382/ab4f03

4. B. C. Lutfuoglu, J. Kriz, S. Zare, and H. Hassanabadi, *Interaction of the magnetic quadrupole moment of a non-relativistic particle with an electric field in the background of screw dislocations with a rotating frame*, Phys. Scr. **96** (2021) 015005. https://doi.org/10.1088/1402-4896/abc78b

5. H. Chen, S. Zare, H. Hassanabadi, and Z. W. Long, *Quantum description of the moving magnetic quadrupole moment interacting with electric field configurations under the rotating background with the screw dislocation*, Ind. J. Phys. **96** (2022) 4219. https://doi.org/10.1007/s12648-022-02328-w

6. S. Zare, H. Hassanabadi, A. Guvendi, and W. S. Chung, *On the interaction of a Cornell-type nonminimal coupling with the scalar field under the background of topological defects*, Int. J. Mod. Phys. A **37** (2022) 2250033. https://doi.org/10.1142/S0217751X22500336

7. S. S. Alves, M. M. Cunha, H. Hassanabadi, and E. O. Silva, *Approximate analytical solutions of the Schrödinger equation with Hulthén potential in the global monopole spacetime*, Universe **9** (2023) 132. https://doi.org/10.3390/universe9030132

8. A. Vilenkin, *Cosmic strings and domain walls*, Phys. Rep. **121** (1985) 263. https://doi.org/10.1016/0370-1573(85)90033-X

9. M. Barriola, and A. Vilenkin, *Gravitational field of a global monopole*, Phys. Rev. Lett. **63** (1989) 341. https://doi.org/10.1103/PhysRevLett.63.341

10. T. Kibble, and A. Srivastava, *Condensed matter analogues of cosmology*, J. Phys.: Cond. Matter **25** (2013) 400301. https://doi.org/10.1088/0953-8984/25/40/400301

11. K. Bakke, C. Furtado, and S. Sergeenkov, *Holonomic quantum computation associated with a defect structure of conical graphene*, EuroPhys. Lett. **87** (2009) 30002. https://doi.org/10.1209/0295-5075/87/30002

12. J. Carvalho, C. Furtado, and F. Moraes, *Dirac oscillator interacting with a topological defect*, Phys. Rev. A **84** (2011) 032109. https://doi.org/10.1103/PhysRevA.84.032109

13. A. Boumali, and N. Messai, *Klein-Gordon oscillator under a uniform magnetic field in cosmic string space-time*, Can. J. Phys. **92** (2014) 1460. https://doi.org/10.1139/cjp-2013-0431

14. R. L. L. Vitória, and K. Bakke, *Relativistic quantum effects of confining potentials on the Klein-Gordon oscillator*, Eur. Phys. J. Plus **131** (2016) 36. https://doi.org/10.1140/epjp/i2016-16036-4

15. Z. Wang, Z. Long, C. Long, and M. Wu, *Relativistic quantum dynamics of a spinless particle in the Som-Raychaudhuri spacetime*, Eur. Phys. J. Plus **130** (2015) 36. https://doi.org/10.1140/epjp/i2015-15036-2

16. R. D. Lambaga, and H. S. Ramadhan, *Gravitational field of global monopole within the Eddington-inspired Born-Infeld theory of gravity*, Eur. Phys. J. C **78** (2018) 436. https://doi.org/10.1140/epjc/s10052-018-5906-x

17. A. Boumali, and H. Aounallah, *Exact solutions of vector bosons in the presence of the Aharonov-Bohm and Coulomb potentials in the gravitational field of topological defects in non-commutative space-time*, Rev. Mex. de Fis. **66** (2020) 192. https://doi.org/10.31349/RevMexFis.66.192

18. E. A. F. Braganca, R. L. L. Vitoria, H. Belich, and E. R. B. de Mello, *Relativistic quantum oscillators in the global monopole spacetime*, Eur. Phys. J. C **80** (2020) 206. https://doi.org/10.1140/epjc/s10052-020-7774-4

19. R. L. L. Vitoria, and H. Belich, *Harmonic oscillator in an environment with a pointlike defect*, Phys. Scr. **94** (2019) 125301. https://doi.org/10.1088/1402-4896/ab3bc1

20. K. Bakke, and C. Furtado, *Analysis of the interaction of an electron with radial electric fields in the presence of a disclination*, Int. J. Geo. Meth. Mod. Phys. **16** (2019) 1950172. https://doi.org/10.1142/S021988781950172X

21. N. Soheibi, M. Hamzavi, M. Eshghi, and S. M. Ikhdair, *Screw dislocation and external fields effects on the Kratzer pseudodot*, Eur. Phys. J. B **90** (2017) 212. https://doi.org/10.1140/epjb/e2017-80468-9

22. C. Filgueiras, M. Rojas, G. Aciole, and E. O. Silva, *2DEG on a cylindrical shell with a screw dislocation*, Phys. Lett. A **379** (2015) 2110. https://doi.org/10.1016/j.physleta.2015.06.035

23. L. C. N. Santosa, and Jr. C. C. Barros, *Relativistic quantum motion of spin-0 particles under the influence of noninertial effects in the cosmic string spacetime*, Eur. Phys. J. C **78** (2018) 13. https://doi.org/10.1140/epjc/s10052-017-5476-3

24. F. Ahmed, *The generalized Klein-Gordon oscillator in the background of cosmic string space-time with a linear potential in the Kaluza-Klein theory*, Eur. Phys. J. C **80** (2020) 211. https://doi.org/10.1140/epjc/s10052-020-7781-5

25. A. Bouzenada, A. Boumali, and F. Serdouk, *Thermal properties of the 2D Klein-Gordon oscillator in a cosmic string space-time*, Theor. Math. Phys. **216** (2023) 1055. https://doi.org/10.1134/S0040577923070115

26. K. Bakke, *Noninertial effects on the Dirac oscillator in a topological defect spacetime*, Eur. Phys. J. Plus, **127** (2012) 82. https://doi.org/10.1140/epjp/i2012-12082-2

27. K. Bakke, and C. Furtado, *On the interaction of the Dirac oscillator with the Aharonov-Casher system in topological defect backgrounds*, Ann. Phys. 336 (2013) 489. https://doi.org/10.1016/j.aop.2013.06.007

28. M. J. Beuno, J. L. de Melo, C. Furtado, and A. M. de M. Carvalho, *Quantum dot in a graphene layer with topological defects*, Eur. Phys. J. Plus, **129** (2014) 201. https://doi.org/10.1140/epjp/i2014-14201-5

29. K. Bakke, and H. Mota, *Dirac oscillator in the cosmic string spacetime in the context of gravity's rainbow*, Eur. Phys. J. Plus, **133** (2018) 409. https://doi.org/10.1140/epjp/i2018-12268-6

30. S. S. Alves, F. dos S. Azevedo, C. Filgueiras, and E. O. Silva, *Exact and approximate bound state solutions of the Schrödinger equation with a class of Kratzer-type potentials in the global monopole spacetime*, Chin. J. Phys. **88** (2024) 609. https://doi.org/10.1016/j.cjph.2023.10.012

31. B. Chakraborty, K. S. Gupta, and S. Sen, *Coulomb screening in graphene with topological defects*, Eur. Phys. J. B **88** (2015) 155. https://doi.org/10.1140/epjb/e2015-60129-y

32. P. Nwabuzor, C. O. Edet, A. N. Ikot, U. S. Okorie, M. Ramantswana, R. Horchani, A. H. Abdel-Aty, and G. J. Rampho, *Analyzing the Effects of Topological Defect (TD) on the Energy Spectra and Thermal Properties of LiH, TiC and I2 Diatomic Molecules*, Entropy **23** (2021) 1060. https://doi.org/10.3390/e23081060

33. C. O. Edet, and A. N. Ikot, *Effects of Topological Defect on the Energy Spectra and Thermo-magnetic Properties of Diatomic Molecule*, J. Low Temp. Phys. **203** (2021) 84. https://doi.org/10.1007/s10909-021-02577-9

34. A. N. Ikot, U. S. Okorie, P. Sawangtong, and R. Horchani, *Effects of Topological Defects and AB Fields on the Thermal Properties, Persistent Currents and Energy Spectra with an Exponential-Type Pseudoharmonic Potential*, Int. J. Theor. Phys. **62** (2023) 197. https://doi.org/10.1007/s10773-023-05453-2

35. L. K. Permatahati, C. Cari, A. Suparmi, and H. Harjana, *Topological effects on relativistic energy spectra of diatomic molecules under the magnetic field with Kratzer potential and thermodynamic-optical properties*, Int. J. Theor. Phys. **62** (2023) 246. https://doi.org/10.1007/s10773-023-05494-7

36. V. Skogvoll, J. Ronning, M. Salvalaglio, and L. Angheluta, *A unified field theory of topological defects and non-linear local excitations*, Comp. Mat. **9** (2023) 122. https://doi.org/10.1038/s41524-023-01077-6

37. O. J. Oluwadare, K. E. Thylwe, and K. J. Oyewumi, *Non-relativistic phase shifts for scattering on generalized radial Yukawa potentials*, Commun. Theor. Phys. **65** (2016) 434. https://doi.org/10.1088/0253-6102/65/4/434

38. O. J. Oluwadare, and K. J. Oyewumi, *The semi-relativistic scattering states of the two-body spinless Salpeter equation with the Varshni potential model*, Eur. Phys. J. Plus **132** (2017) 277. https://doi.org/10.1140/epjp/i2017-11549-x

39. O. J. Oluwadare, and K. J. Oyewumi, *Scattering states solutions of Klein-Gordon equation with three physically solvable potential models*, Chin. J. Phys. **55** (2017) 2422. https://doi.org/10.1016/j.cjph.2017.10.007

40. A. N. Ikot, U. S. Okorie, G. J. Rampho, C. O. Edet, R. Horchani, A. Abdel-Aty, N. A. Alshehri, and S. K. Elagan, *Bound and scattering state solutions of the Klein-Gordon equation with Deng-Fan potential in higher dimensions*, Few-Body Syst. **62** (2021) 101. https://doi.org/10.1007/s00601-021-01693-2

41. U. S. Okorie, A. N. Ikot, G. J. Rampho, M. C. Onyeaju, M. U. Ibezim-Ezeani, A. Abdel-Aty, and M. Ramantswana, *Bound and scattering states of the Klein-Gordon equation for shifted Tietz-Wei potential with applications to diatomic molecules*, Mol. Phys. **119** (2021) e1922773. https://doi.org/10.1080/00268976.2021.1922773

42. U. S. Okorie, A. N. Ikot, C. O. Edet, G. J. Rampho, R. Horchani, and H. Jelessi, *Bound and scattering states solutions of the Klein-Gordon equation with generalized Mobius square potential in D-dimensions*, Eur. Phys. J. D **75** (2021) 53. https://doi.org/10.1140/epjd/s10053-021-00059-x

43. S. S. Alves, M. M. Cunha, H. Hassanabadi, and E. O. Silva, *Approximate analytical solutions of the Schrödinger equation with Hulthén potential in the global monopole spacetime*, Universe **9** (2023) 132. https://doi.org/10.3390/universe9030132

44. C. O. Edet, and P. O. Okoi, *Any l-state solutions of the Schrödinger equation for q-deformed Hulthen plus generalized inverse quadratic Yukawa potential in arbitrary dimensions*, Rev. Mex. Fis. **65** (2019) 333. https://doi.org/10.31349/RevMexFis.65.333

45. C. A. Onate, O. Ebomwonyi, K. O. Dopamu, J. O. Okoro, and M. O. Oluwayemi, *Eigen solutions of the D-dimensional Schrödinger equation with inverse trigonometry scarf potential and Coulomb potential*, Chin. J. Phys. **56** (2018) 2538. https://doi.org/10.1016/j.cjph.2018.03.013

46. E. S. William, E. P. Inyang, and E. A. Thompson, *Arbitrary l-solutions of the Schrödinger equation interacting with Hulthén-Hellmann potential model*, Rev. Mex. de Fis. **66** (2020) 730. https://doi.org/10.31349/RevMexFis.66.730

47. F. Ahmed, *Topological effects produced by point-like global monopole with Hulthen plus screened Kratzer potential on Eigenvalue solutions and NU-method*, Phys. Scr. **98** (2023) 015403. https://doi.org/10.1088/1402-4896/aca6b3

48. R. L. Greene, and C. Aldrich, *Variational wave functions for a screened Coulomb potential*, Phys. Rev. A **14** (1976) 2363. https://doi.org/10.1103/PhysRevA.14.2363

49. A. K. Bhatia, *Scattering and Its Applications to Various Atomic Processes: Elastic Scattering, Resonances, Photoabsorption, Rydberg States, and Opacity of the Atmosphere of the Sun and Stellar Objects*, Atoms **8** (2020) 78. https://doi.org/10.3390/atoms8040078

50. A. K. Bhatia, *Photodetachment of the positronium negative ion with excitation in the positronium atom*, Mod. Concepts Mat. Sci. **1** (2020) 1. https://doi.org/10.3390/atoms7010002

51. A. K. Bhatia, *Photodetachment of the positronium negative ion with excitation in the positronium atom*, Atoms **7** (2018) 2. https://doi.org/10.33552/MCMS.2020.03.000553

52. A. N. Ikot, U. S. Okorie, P. O. Amadi, C. O. Edet, G. J. Rampho, and R. Sever, *The Nikiforov-Uvarov-Functional Analysis (NUFA) Method: A new approach for solving exponential-type potentials*, Few-Body Syst. **62** (2021) 9. https://doi.org/10.1007/s00601-021-01593-5

53. A. F. Nikiforov, and V. B. Uvarov, *Special Functions of Mathematical Physics*, Birkhauser, Basel (1988).

54. C. Tezcan, and R. Sever, *A general approach for the exact solution of the Schrödinger equation*, Int. J. Theor. Phys. **48** (2008) 337. https://doi.org/10.1007/s10773-008-9806-y

55. B. J. Falaye, K. J. Oyewumi, S. M. Ikhdair, and M. Hamzavi, *Eigensolution techniques, their applications and Fishers information entropy of the Tietz-Wei diatomic molecular model*, Phys. Scr. **89** (2014) 115204. https://doi.org/10.1088/0031-8949/89/11/115204